(Preprint) AAS 09-202

EXTENDED KALMAN FILTER FOR MMS STATE ESTIMATION

Julie K. Thienel*, F. Landis Markley†, and Richard R. Harman‡

The Magnetospheric MultiScale Mission is a four spacecraft formation flying mission designed to study the Earth's magnetosphere. The spacecraft fly in highly elliptical orbits, forming a tetrahedron at apogee. Each spacecraft spins at 3 RPM and is equipped with a star scanner, slit sun sensor, and accelerometer. The purpose of this work is to develop an Extended Kalman Filter to simultaneously estimate the attitude, angular velocity, angular acceleration, and center of mass of each spacecraft.

INTRODUCTION

The Magnetospheric Multiscale (MMS) mission employs four identical spacecraft to study the Earth's magnetosphere.[1] The spacecraft will fly in highly elliptical orbits, the semi-major axes of which are approximately 42,000 km with an eccentricity of 0.8. Through slight variations between the orbital elements of each spacecraft, the orbits are such that the four spacecraft form a tetrahedron at apogee.[2]

The spacecraft are spin stabilized with a spin rate of 3 rpm. Each is equipped with redundant star sensors, 3 orthogonal accelerometers, and slit sun sensors. There are four major configurations of the spacecraft. The first has all extendable booms stowed, second has all booms fully deployed, and two are different combinations of booms deployed and stowed. Each spacecraft is equipped with eight 20 N thrusters to provide a thrust force in the spacecraft radial direction and four 5 N thrusters parallel to the spin axis. Precise maneuvers are required for each spacecraft in order to establish the correct orbital elements that will result in the tetrahedron formation at apogee. Knowledge of the center of mass location is crucial in the maneuver planning to avoid unwanted torques and minimize fuel usage. In this work, an Extended Kalman Filter (EKF) is presented which will estimate the center of mass along with the spacecraft attitude, angular velocity, and angular acceleration. The algorithm utilizes measured quaternions from the star sensor, a measurement of the spin rate from the slit sun sensor, and accelerometer data. The inertia matrix is assumed to be measured on the ground, based on a measured center of mass. The true inertia matrix is related to the measured inertia through the parallel axis theorem, which provides the relationship between the center of mass and the attitude dynamics. The accelerometer produces a measurement of the non-gravitational acceleration of the spacecraft at the location of the accelerometer. The non-gravitational acceleration comprises the rotational acceleration of the accelerometer (the accelerometer is not located at the center of mass) plus the non-gravitational acceleration of the center of mass from sources such as drag and thruster firings.

*Assistant Professor, U.S. Naval Academy, Department of Aerospace Engineering, Annapolis, MD, 21402, thienel@usna.edu.
†Aerospace Engineer, NASA Goddard Space Flight Center, GN&C Systems Engineering Branch, Greenbelt, MD, 20771, landis.markley@nasa.gov.
‡Aerospace Engineer, NASA Goddard Space Flight Center, Mission Validation and Operations Branch, Greenbelt, MD, 20771, richard.r.harman@nasa.gov.

The EKF is tested with a simulation of a single MMS spacecraft. The spacecraft is spinning about the body z axis, with added nutation. No non-gravitational (contact) forces are applied, however a disturbance torque from solar pressure is included in the truth model. The other sources of error are sensor noise and uncertainty in the state elements. The accelerometer model is expanded to include a bias and the final tests include the estimation of the accelerometer bias.

First the mathematical development of the EKF is presented, followed by results from several scenarios in which the spacecraft inertia, accelerometer location, center of mass location, and angular velocity are varied.

EXTENDED KALMAN FILTER DEVELOPMENT

The filter state is given as

$$\boldsymbol{X} = \begin{bmatrix} \boldsymbol{q} \\ \boldsymbol{\omega} \\ \dot{\boldsymbol{\omega}} \\ \boldsymbol{r}_c \\ \boldsymbol{a}_b \end{bmatrix}$$

where $\boldsymbol{q}$ is the attitude quaternion, $\boldsymbol{\omega}$ is the angular velocity in body coordinates, $\dot{\boldsymbol{\omega}}$ is the angular acceleration in body coordinates, $\boldsymbol{r}_c$ is the location of the center of mass in body coordinates, and $\boldsymbol{a}_b$ is an accelerometer bias, also in body coordinates. The error state is defined as

$$\boldsymbol{x} = \begin{bmatrix} \boldsymbol{\alpha} \\ \Delta\boldsymbol{\omega} \\ \Delta\dot{\boldsymbol{\omega}} \\ \Delta\boldsymbol{r}_c \\ \Delta\boldsymbol{a}_b \end{bmatrix}$$

where $\boldsymbol{\alpha}$ is given as the first three components of the error quaternion representation[3]

$$\delta\boldsymbol{q}(\boldsymbol{\alpha}) \approx \begin{bmatrix} \boldsymbol{\alpha}/2 \\ 1 \end{bmatrix}$$

Measurement Models

Star Sensor. The star sensor provides a measurement of the quaternion, $\boldsymbol{q}_{obs}$. The measurement of the attitude error, $\boldsymbol{\alpha}$, is obtained with the a priori quaternion estimate and the measured quaternion as[3]

$$\delta\boldsymbol{q}(\boldsymbol{\alpha}_{obs}) = \boldsymbol{q}_{obs} \otimes \hat{\boldsymbol{q}}(-)^{-1}$$

$$\boldsymbol{\alpha}_{obs} = 2\delta\boldsymbol{q}(\boldsymbol{\alpha}_{obs})_{1:3}\text{sign}(\delta\boldsymbol{q}(\boldsymbol{\alpha}_{obs})_4)$$

The measurement residual, $\boldsymbol{\rho}$, is

$$\boldsymbol{\rho} = \boldsymbol{\alpha}_{obs}$$

There is no 'estimated' measurement in this case since the updated attitude error state is incorporated into the updated quaternion, a process known as 'reset'.

The measurement matrix used in the EKF is simply

$$H_q = \begin{bmatrix} \text{I} & 0_{3x9} \end{bmatrix}$$

where I is a 3x3 identity matrix.

Slit Sun Sensor. The sun sensor provides two measurements. The first is the sun vector in body coordinates

$$\boldsymbol{s}_b = \begin{bmatrix} \sin\phi\cos\psi \\ \sin\phi\sin\psi \\ \cos\phi \end{bmatrix}$$

where ϕ is the measured angle between the spin axis ($\boldsymbol{z}_b$) and the sun direction, ψ is the fixed angle between the sun sensor slit and the spacecraft body x, y plane.[4] The sun vector in inertial coordinates is related to the vector in body coordinates as

$$\boldsymbol{s}_b = A(\boldsymbol{q})\boldsymbol{s}_i + \nu_s \tag{1}$$

where $A(\boldsymbol{q})$ is the attitude matrix, representing the transformation from inertial to body coordinates, and ν_s is zero-mean, white measurement noise. The measurement residual is

$$\boldsymbol{\rho} = \boldsymbol{s}_b - A(\hat{\boldsymbol{q}}(-))\boldsymbol{s}_i$$

The measurement matrix for the sun sensor is[3]

$$H_s = \begin{bmatrix} [\boldsymbol{s}_b\times] & 0_{3x12} \end{bmatrix}$$

H_s is derived by linearizing equation 1.

The sun sensor also provides the time between successive sun sightings through the slit. Let

$$\omega_z = \frac{d\theta_z}{dt} \tag{2}$$

where ω_z is the angular velocity about the z body axis, or spin axis. Integrating equation 2

$$\theta_z(t_j) - \theta_z(t_{j-1}) = \int_{t_{j-1}}^{t_j} \omega_z(t)dt$$

where t_j indicates the current time and t_{j-1} is the time of the last sun crossing. Or, to first order

$$\theta_z(t_j) - \theta_z(t_{j-1}) = \omega_z(t_{j-1})(t_j - t_{j-1}) + \nu_t$$

where ν_t represents the error, which will be treated simply as zero-mean white measurement noise. Between successive sun sightings, the z axis travels through 360 degrees, or

$$2\pi = \omega_z(t_{j-1})(t_j - t_{j-1}) + \nu_t$$

Here the measurement residual is

$$\boldsymbol{\rho} = 2\pi - \hat{\omega}_{z,j-1}(t_j - t_{j-1})$$

where $\hat{\omega}_{z,j-1}$ represents the estimate of $\omega_z(t_{j-1})$. The measurement matrix is

$$H_{spin} = \begin{bmatrix} 0_{1x3} & 0 & 0 & (t_j - t_{j-1}) & 0_{1x9} \end{bmatrix}$$

Alternatively, the angle θ_z at time t_j could be modeled using a Taylor series as

$$\theta_z(t_j) = \theta_z(t_{j-1}) + \omega_z(t_j - t_{j-1}) + \frac{1}{2}\dot{\omega}_z(t_j - t_{j-1})^2 + H.O.T \tag{3}$$

Or

$$2\pi = \begin{bmatrix} (t_j - t_{j-1}) & \frac{1}{2}(t_j - t_{j-1})^2 \end{bmatrix} \begin{bmatrix} \omega_z \\ \dot{\omega}_z \end{bmatrix} + \nu_t$$

Here the residual becomes

$$\boldsymbol{\rho} = 2\pi - [(t_j - t_{j-1})\hat{\omega}_{z,j-1} + \frac{1}{2}(t_j - t_{j-1})^2\dot{\hat{\omega}}_{z,j-1}]$$

and the measurement matrix is

$$H_{spin} = \begin{bmatrix} 0_{1x3} & 0 & 0 & (t_j - t_{j-1}) & 0 & 0 & \frac{1}{2}(t_j - t_{j-1})^2 & 0_{1x6} \end{bmatrix}$$

The higher order terms in equation 3 are again simply treated as zero-mean white measurement noise, given as ν_t.

Accelerometer. Figure 1 depicts the relationship between the true center of mass, the accelerometer, and the measured location of the center of mass. Let $\boldsymbol{r}$ be the position vector of the accelerometer from the true center of mass to the accelerometer, $\boldsymbol{r}_A$ be the measured position vector of the accelerometer, and $\boldsymbol{r}_c$ be the unknown position vector from the true center of mass to the measured center of mass. The acceleration of the accelerometer is[5]

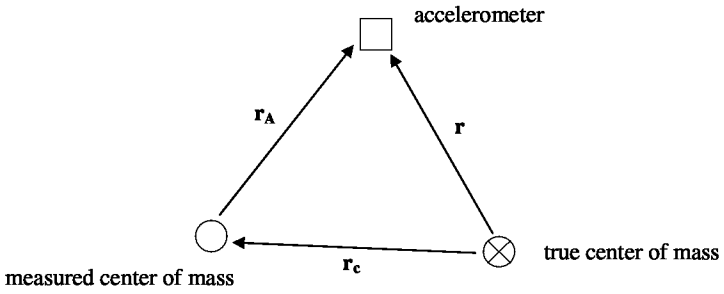

Figure 1. Location of Accelerometer, Measured Center of Mass, and True Center of Mass

$$\boldsymbol{a} = [\dot{\boldsymbol{\omega}}\times]\boldsymbol{r} + [\boldsymbol{\omega}\times]^2\boldsymbol{r} + \boldsymbol{a}_o \tag{4}$$

$$\boldsymbol{a} = \boldsymbol{a}_{rot} + \boldsymbol{a}_o$$

where $\boldsymbol{r} = \boldsymbol{r}_c + \boldsymbol{r}_A$. The acceleration of the center of mass is $\boldsymbol{a}_o$, written as a sum of both gravitational and non-gravitational acceleration terms.

$$\boldsymbol{a}_o = \boldsymbol{a}_g + \boldsymbol{a}_{ng}$$

where $\boldsymbol{a}_g$ is the acceleration due to gravity and $\boldsymbol{a}_{ng}$ is the acceleration of the center of mass due to non-gravitational forces such as drag, thrusters, etc.

Three accelerometers measure the three non-gravitational components of $\boldsymbol{a}$ along each body axis. The measured acceleration is assumed to be related to the true acceleration as

$$\boldsymbol{a}_m = \boldsymbol{a} - \boldsymbol{a}_g + \boldsymbol{a}_b + \nu_a = \boldsymbol{a}_{rot} + \boldsymbol{a}_{ng} + \boldsymbol{a}_b + \nu_a \tag{5}$$

where $\boldsymbol{a}_b$ is an accelerometer bias and ν_a is zero-mean, white measurement noise.

If the non-gravitational accelerations from contact forces are known, or can be modelled, a measurement of the rotational acceleration can be written as

$$\boldsymbol{a}_{rot,m} = \boldsymbol{a}_m - \boldsymbol{a}_{ng} = \boldsymbol{a}_{rot} + \boldsymbol{a}_b + \nu_a \tag{6}$$

Equation 6 is linearized with respect to the components of the state vector, neglecting higher order terms

$$\boldsymbol{a}_{rot,m} = \boldsymbol{a}_{rot,m}\big|_{\hat{\boldsymbol{X}}} + \frac{\partial \boldsymbol{a}_{rot,m}}{\partial \boldsymbol{X}}\big|_{\hat{\boldsymbol{X}}} \boldsymbol{x} + \nu_a$$

The residual is

$$\boldsymbol{\rho} = \boldsymbol{a}_{rot,m} - \hat{\boldsymbol{a}}_{rot}$$

where $\hat{\boldsymbol{a}}_{rot} = \boldsymbol{a}_{rot,m}\big|_{\hat{\boldsymbol{X}}}$ is computed using the estimated state components in equation 6.

The accelerometer measurement matrix is

$$H_{acc} = \frac{\partial \boldsymbol{a}_{rot,m}}{\partial \boldsymbol{X}}\big|_{\hat{\boldsymbol{X}}} = \left[\begin{array}{cccc} 0_{3x3} & H_{a,\omega} & H_{a,\dot{\boldsymbol{\omega}}} & H_{a,\boldsymbol{r}_c} \end{array} \quad \mathrm{I}_{3\times 3} \right] \Big|_{\hat{\boldsymbol{X}}}$$

where

$$H_{a,\omega} = \begin{bmatrix} \omega_y r_y + \omega_z r_z & \omega_x r_y - 2\omega_y r_x & \omega_x r_z - 2\omega_z r_x \\ \omega_y r_x - 2\omega_x r_y & \omega_x r_x + \omega_z r_z & \omega_y r_z - 2\omega_z r_y \\ \omega_z r_x - 2\omega_x r_z & \omega_z r_y - 2\omega_y r_z & \omega_x r_x + \omega_y r_y \end{bmatrix}$$

$$H_{a,\dot{\boldsymbol{\omega}}} = -[\boldsymbol{r}\times]$$

$$H_{a,\boldsymbol{r}_c} = [\dot{\boldsymbol{\omega}}\times] + [\boldsymbol{\omega}\times]^2$$

where (r_x, r_y, r_z) are the components of $\boldsymbol{r} = \boldsymbol{r}_A + \boldsymbol{r}_c$, $[\boldsymbol{r}\times]$ is a skew symmetric matrix composed of the elements of $\boldsymbol{r}$, and $(\omega_x, \omega_y, \omega_z)$ are the components of $\boldsymbol{\omega}$. H_{acc} is evaluated with the current estimates of the state elements, $\hat{\boldsymbol{\omega}}_k(-)$, $\hat{\dot{\boldsymbol{\omega}}}$, $\hat{\boldsymbol{r}}_c$.

EKF Measurement Update

The state is updated with each measurement given above when the measurement is available. If the measurements are not simultaneous, the state and covariance are propagated to the next measurement time point. If the measurements are available simultaneously (the sun vector and measured spin rate, for example), the measurements can be updated sequentially (with a zero-time propagation between).

The EKF measurement update procedure is as follows. First, the Kalman gain matrix is computed at the given time point, k, as

$$\mathrm{K}_k = \mathrm{P}_k(-)\mathrm{H}_k^T(\mathrm{H}_k\mathrm{P}_k(-)\mathrm{H}_k^T + \mathrm{R})^{-1}$$

where $P_k(-)$ is the a priori covariance matrix. R is the measurement noise covariance matrix for the given sensor. The matrix H_k is defined above for each of the measurement types. H_k is evaluated with the current state $\hat{\boldsymbol{X}}_k(-)$. The updated error state is formed as

$$\hat{\boldsymbol{x}}_k(+) = \mathrm{K}_k\boldsymbol{\rho}_k$$

A delta quaternion is formed as[3]

$$\delta \boldsymbol{q}_k(\hat{\boldsymbol{x}}(+)) = \frac{1}{2}\begin{bmatrix} \hat{\boldsymbol{x}}_{k,1:3}(+) \\ \sqrt{4 - \hat{\boldsymbol{x}}_{k,1:3}^T \hat{\boldsymbol{x}}_{k,1:3}(+)} \end{bmatrix}$$

Note that $\hat{\boldsymbol{x}}_{k,1:3}(+)$ refers to the first three elements of $\hat{\boldsymbol{x}}_k(+)$, the attitude error components. The updated attitude quaternion is then computed as

$$\hat{\boldsymbol{q}}_k(+) = \delta \boldsymbol{q}_k(\hat{\boldsymbol{x}}_k(+)) \otimes \hat{\boldsymbol{q}}_k(-)$$

The remaining states are updated as

$$\hat{\boldsymbol{X}}_k(+) = \hat{\boldsymbol{X}}_k(-) + \hat{\boldsymbol{x}}_k(+)$$

The covariance matrix is updated as

$$\mathrm{P}_k(+) = (\mathrm{I} - \mathrm{K}_k\mathrm{H}_k)\mathrm{P}_k(-)(\mathrm{I} - \mathrm{K}_k\mathrm{H}_k)^T + \mathrm{K}_k\mathrm{R}\mathrm{K}_k^T$$

where symmetry of the covariance matrix is forced by

$$\mathrm{P}_k(+) = \frac{1}{2}(\mathrm{P}_k(+) + \mathrm{P}_k(+)^T)$$

Propagation

The quaternion kinematic equation is given as

$$\dot{\boldsymbol{q}} = \frac{1}{2}Q(\boldsymbol{q})\boldsymbol{\omega} \tag{7}$$

The quaternion is propagated numerically using equation 7, using the current estimate of the rate $\hat{\boldsymbol{\omega}} = \hat{\boldsymbol{\omega}}_k(+)$ and quaternion $\hat{\boldsymbol{q}} = \hat{\boldsymbol{q}}_k(+)$.

Euler's equation is given as

$$\dot{\boldsymbol{\omega}} = \mathrm{J}^{-1}[\mathrm{J}\boldsymbol{\omega}\times]\boldsymbol{\omega} + \mathrm{J}^{-1}\boldsymbol{T} \tag{8}$$

where $\boldsymbol{T}$ are external torques and J is the spacecraft inertia matrix about the true center of mass. J is assumed to be constant. If the spacecraft configuration is changing, or the mass is changing due to thruster firings, then J would not be constant. Let $\mathrm{J_B}$ represent a known inertia matrix, measured on the ground with respect to the measured center of mass. The true inertia matrix is related to the measured inertia matrix through the parallel axis theorem

$$\mathrm{J} = \mathrm{J_B} - m[\boldsymbol{r}_c\times]^2 = (\mathrm{I} - m[\boldsymbol{r}_c\times]^2\mathrm{J_B}^{-1})\mathrm{J_B} \tag{9}$$

where m is the mass of the spacecraft. From reference [6], the inverse of a rank two matrix plus an identity matrix is given as

$$(\mathrm{I} + \mathrm{G})^{-1} = \mathrm{I} - \frac{1}{a+b}(a\mathrm{G} - \mathrm{G}^2)$$

where

$$a = 1 + trace(\mathrm{G})$$

and

$$2b = (trace(\mathrm{G}))^2 - trace(\mathrm{G}^2)$$

Here G has rank two and is written as

$$\mathrm{G} = -m[\boldsymbol{r}_c\times]^2 {\mathrm{J_B}}^{-1}$$

J^{-1} is then written as

$$\mathrm{J}^{-1} = {\mathrm{J_B}}^{-1}(\mathrm{I} - \frac{1}{a+b}(a\mathrm{G} - \mathrm{G}^2)) = {\mathrm{J_B}}^{-1}(\mathrm{I} - \mathrm{J}_{\boldsymbol{r}_c}) \tag{10}$$

where $\mathrm{J}_{\boldsymbol{r}_c} = \frac{1}{a+b}(a\mathrm{G} - \mathrm{G}^2)$. Equation 8 is used to propagate the rate numerically using current state estimates. Equation 10 can be used to calculate the estimated J^{-1} since ${\mathrm{J_B}}^{-1}$ can be computed once initially, and then no additional matrix inversions are needed.

Next, equation 8 is differentiated to obtain an expression for $\ddot{\boldsymbol{\omega}}$

$$\ddot{\boldsymbol{\omega}} = \mathrm{J}^{-1}\left[[\mathrm{J}\dot{\boldsymbol{\omega}}\times]\boldsymbol{\omega} + [\mathrm{J}\boldsymbol{\omega}\times]\dot{\boldsymbol{\omega}} + \dot{\mathbf{T}}\right] \tag{11}$$

As with the previous states, equation 11 is used to propagate the angular acceleration numerically, using current state estimates where needed and a model of $\dot{\mathbf{T}}$ if any external torques are modeled.

Finally, the location of the center of mass and the accelerometer bias are both modeled as constant

$$\dot{\boldsymbol{r}}_c = 0$$

$$\dot{\boldsymbol{a}}_b = 0$$

If the mass is changing, the center of mass can change and a more suitable model applied for $\dot{\boldsymbol{r}}_c$.

Next the models for propagating each of the error states are presented. The linear EKF approximation of $\dot{\boldsymbol{\alpha}}$ is given as[3]

$$\dot{\boldsymbol{\alpha}} = -[\hat{\boldsymbol{\omega}}\times]\boldsymbol{\alpha} + \Delta\boldsymbol{\omega} \tag{12}$$

The equation for the error state, $\Delta\ddot{\boldsymbol{\omega}}$, is

$$\Delta\ddot{\boldsymbol{\omega}} = \frac{\partial\ddot{\boldsymbol{\omega}}}{\partial\boldsymbol{X}}\Big|_{\hat{\boldsymbol{X}}}\boldsymbol{x} + \boldsymbol{\gamma}_{\ddot{\boldsymbol{\omega}}}$$

where $\boldsymbol{\gamma}_{\ddot{\boldsymbol{\omega}}}$ represents the higher order terms in the expansion. Let

$$\frac{\partial\ddot{\boldsymbol{\omega}}}{\partial\boldsymbol{X}}\Big|_{\hat{\boldsymbol{X}}} = \begin{bmatrix} \mathrm{F}_{\ddot{\boldsymbol{\omega}},\boldsymbol{\alpha}} & \mathrm{F}_{\ddot{\boldsymbol{\omega}},\boldsymbol{\omega}} & \mathrm{F}_{\ddot{\boldsymbol{\omega}},\dot{\boldsymbol{\omega}}} & \mathrm{F}_{\ddot{\boldsymbol{\omega}},\boldsymbol{r}_c} & \mathrm{F}_{\ddot{\boldsymbol{\omega}},\boldsymbol{a}_b} \end{bmatrix}\Big|_{\hat{\boldsymbol{X}}}$$

Let $\mathrm{F}_{\ddot{\boldsymbol{\omega}},\boldsymbol{\alpha}} = \mathrm{F}_{\ddot{\boldsymbol{\omega}},\boldsymbol{a}_b} = 0$.

$$\mathrm{F}_{\ddot{\boldsymbol{\omega}},\boldsymbol{\omega}} = \frac{\partial\ddot{\boldsymbol{\omega}}}{\partial\boldsymbol{\omega}} = \mathrm{J}^{-1}\left[[\mathrm{J}\dot{\boldsymbol{\omega}}\times] - [\dot{\boldsymbol{\omega}}\times]\mathrm{J}\right]$$

$$\mathrm{F}_{\ddot{\boldsymbol{\omega}},\dot{\boldsymbol{\omega}}} = \frac{\partial\ddot{\boldsymbol{\omega}}}{\partial\dot{\boldsymbol{\omega}}} = \mathrm{J}^{-1}\left[[\mathrm{J}\boldsymbol{\omega}\times] - [\boldsymbol{\omega}\times]\mathrm{J}\right]$$

Substituting equation 9 into 11

$$\begin{aligned}\ddot{\boldsymbol{\omega}} &= \mathrm{J}^{-1}\left[[-\boldsymbol{\omega}\times]\mathrm{J}\dot{\boldsymbol{\omega}} + [-\dot{\boldsymbol{\omega}}\times]\mathrm{J}\boldsymbol{\omega} + \dot{\mathbf{T}}\right] = \mathrm{J}^{-1}\left[[-\boldsymbol{\omega}\times](\mathrm{J_B} - m[\boldsymbol{r}_c\times]^2)\dot{\boldsymbol{\omega}} + [-\dot{\boldsymbol{\omega}}\times](\mathrm{J_B} - m[\boldsymbol{r}_c\times]^2)\boldsymbol{\omega} + \dot{\mathbf{T}}\right] \\ &= \mathrm{J}^{-1}\left[[\mathrm{J_B}\dot{\boldsymbol{\omega}}\times]\boldsymbol{\omega} + [\mathrm{J_B}\boldsymbol{\omega}\times]\dot{\boldsymbol{\omega}} + m([\boldsymbol{\omega}\times][\boldsymbol{r}_c\times]^2\dot{\boldsymbol{\omega}} + [\dot{\boldsymbol{\omega}}\times][\boldsymbol{r}_c\times]^2\boldsymbol{\omega}) + \dot{\mathbf{T}}\right]\end{aligned} \tag{13}$$

Substituting equation 10 into 13 gives

$$\ddot{\boldsymbol{\omega}} = \mathrm{J_B}^{-1}(\mathrm{I} - \mathrm{J}_{\boldsymbol{r}_c}) \left[[\mathrm{J_B}\dot{\boldsymbol{\omega}}\times]\boldsymbol{\omega} + [\mathrm{J_B}\boldsymbol{\omega}\times]\dot{\boldsymbol{\omega}} + m([\boldsymbol{\omega}\times][\boldsymbol{r}_c\times]^2\dot{\boldsymbol{\omega}} + [\dot{\boldsymbol{\omega}}\times][\boldsymbol{r}_c\times]^2\boldsymbol{\omega}) + \dot{\mathbf{T}} \right]$$

The matrix $\mathrm{F}_{\ddot{\boldsymbol{\omega}},\boldsymbol{r}_c}$ is then

$$\mathrm{F}_{\ddot{\boldsymbol{\omega}},\boldsymbol{r}_c} = \mathrm{J_B}^{-1}\frac{\partial}{\partial \boldsymbol{r}_c}\left[\mathrm{J}_{\boldsymbol{r}_c}[\boldsymbol{\omega}\times]\mathrm{J_B}\dot{\boldsymbol{\omega}} + [\dot{\boldsymbol{\omega}}\times]\mathrm{J_B}\boldsymbol{\omega}\right] + m\mathrm{J_B}^{-1}\frac{\partial}{\partial \boldsymbol{r}_c}\left[(\mathrm{I} - \mathrm{J}_{\boldsymbol{r}_c})[[\boldsymbol{\omega}\times][\boldsymbol{r}_c\times]^2\dot{\boldsymbol{\omega}} + [\dot{\boldsymbol{\omega}}\times][\boldsymbol{r}_c\times]^2\boldsymbol{\omega}]\right]$$

assuming that $\frac{\partial \dot{\mathbf{T}}}{\partial \boldsymbol{r}_c} = 0$ since no external torques are modeled. Appendix A contains the detailed computations of the above partial derivatives.

Finally, all the error state differential equations are augmented resulting in

$$\dot{\boldsymbol{x}} = \mathrm{F}\boldsymbol{x} + \boldsymbol{\gamma}$$

The error dynamics matrix, F, is given as

$$\mathrm{F} = \begin{bmatrix} -[\hat{\boldsymbol{\omega}}\times] & \mathrm{I} & 0 & 0 & 0 \\ 0 & 0 & \mathrm{I} & 0 & 0 \\ 0 & \mathrm{F}_{\ddot{\boldsymbol{\omega}},\boldsymbol{\omega}} & \mathrm{F}_{\ddot{\boldsymbol{\omega}},\dot{\boldsymbol{\omega}}} & \mathrm{F}_{\ddot{\boldsymbol{\omega}},\boldsymbol{r}_c} & 0 \\ 0 & 0 & 0 & 0 & 0 \\ 0 & 0 & 0 & 0 & 0 \end{bmatrix}$$

The term $\boldsymbol{\gamma}$ represents the inaccuracies in modeling the error dynamics.

The matrix F is assumed to be constant over the short propagation time interval, Δt. The state transition matrix at time t_k is then approximated as

$$\Phi_k = \mathrm{e}^{\mathrm{F}_k \Delta t} \approx \mathrm{I} + \mathrm{F}_k \Delta t$$

The error state propagation is modeled discretely as

$$\boldsymbol{x}_{k+1} = \Phi_k \boldsymbol{x}_k + \boldsymbol{w}_k$$

where $\boldsymbol{w}_k$ is a zero-mean, white sequence added to account for the modeling errors represented above by $\boldsymbol{\gamma}$ and to provide filter stability.[7] The covariance matrix is propagated discretely with

$$\mathrm{P}(-)_{k+1} = \Phi_k \mathrm{P}_k(+)\Phi_k^T + \mathrm{Q}_k$$

where

$$\mathrm{Q}_k = E[\boldsymbol{w}_k \boldsymbol{w}_k^T]$$

Additional Comments

Note that if the star sensor is not available, the attitude is not fully observable with only the sun sensor. Also, without the star sensor the angular velocity and angular acceleration would not be fully observable. As shown in equation 5, the acceleration is coupled with the angular velocity and angular acceleration. Without knowledge of $\boldsymbol{\omega}$ and $\dot{\boldsymbol{\omega}}$, $\boldsymbol{r}_c$ is also not fully observable from the accelerometer measurement.

Table 1. Orbital Elements

Element	Value
semi-major axis	42095.7 km
eccentricity	0.81818
inclination	27.8 deg
argument of perigee	15.0 deg
right ascension of the ascending node	0 deg
true anomaly	180 deg

Note that the precession (ψ), nutation (β), and spin or phase (σ) angles can be extracted from the estimated quaternion[4]

$$\psi = \tan^{-1} \frac{q_2 q_3 - q_1 q_4}{q_1 q_3 + q_2 q_4}$$

$$\beta = \cos^{-1}(-q_1^2 - q_2^2 + q_3^2 + q_4^2)$$

$$\sigma = \tan^{-1} \frac{q_2 q_3 + q_1 q_4}{q_2 q_4 - q_1 q_3}$$

The spin vector expressed in the inertial coordinate system can then be computed as

$$\boldsymbol{l}_{spin,I}^T = \begin{bmatrix} \cos\psi \sin\beta & \sin\psi \sin\beta & \cos\beta \end{bmatrix}$$

or equivalently

$$\boldsymbol{l}_{spin,I}^T = \begin{bmatrix} 2(q_1 q_3 + q_2 q_4) & 2(q_2 q_3 - q_1 q_4) & -q_1^2 - q_2^2 + q_3^2 + q_4^2 \end{bmatrix}$$

RESULTS

The EKF is tested with a simulation of a single MMS spacecraft. The orbital parameters are given in Table 1. The spacecraft mass is 1171 kg and two inertia configurations are considered. The height of each spacecraft is 1.0 m and the diameter is 1.5 m. Table 2 lists the two inertia configurations. J_1 is the inertia for the spacecraft configuration with all booms stowed, and J_2 is the inertia with all booms fully extended.[8]

Table 2. MMS Inertia Matrices (kg-m^2)

J_1			J_2		
783.35	-12.28	-4.84	3160.32	225.92	-4.82
-12.28	803.79	-7.67	225.92	3135.18	-7.42
-4.84	-7.67	1332.99	-4.82	-7.42	5475.89

The results of several test scenarios are presented. In each scenario, the true initial angular velocity is constructed with the following

$$\boldsymbol{\omega} = \begin{bmatrix} 3|\sin\kappa|\boldsymbol{u}_{xy} \\ 3\cos\kappa \end{bmatrix} \text{rpm} \tag{14}$$

where κ is the coning angle, selected from a normal distribution with zero mean and a standard deviation of 0.2 deg. The vector $\boldsymbol{u}_{xy}$ is the unit vector direction of the angular velocity in the x-y plane, constructed from a uniform distribution. The magnitude of the angular velocity vector is 3 rpm. The initial angular acceleration is calculated using equation 8 with the initial angular velocity and inertia. The sun sensor is used only to provide the timing measurement related to ω_{bz}. The three components of the true center of mass location, $\boldsymbol{r}_c$, are selected from a normal distribution, with zero mean and a standard deviation of 5 cm. The accelerometer is located at

$$\boldsymbol{r}_A = \begin{bmatrix} 0.75 & 0.75 & 0.5 \end{bmatrix} \; m$$

The other simulation and filter parameters are given in Table 3. Note that the covariance and process noise values are the values on the main diagonal of each respective matrix for the particular element given. The measurement noise matrices are constructed from the square of the standard deviations given for each sensor. Two sets of standard deviations for the star sensor noise components are considered. The true attitude is initialized such that the y body axis points towards the sun, with the z body axis parallel to the north ecliptic pole. The first test scenario provides a comparison of

Table 3. Initial Conditions

Parameter	Value	Parameter	Value
$\boldsymbol{q}$	$[0.0183, 0.2026, -0.9751, 0.0880]$	$\hat{\boldsymbol{q}}$	$[0, 0, 0, 1]$
$\boldsymbol{\omega}$	random as described	$\hat{\boldsymbol{\omega}}$	$[0, 0, 0]$ deg/sec
$\dot{\boldsymbol{\omega}}$	calculated as described	$\hat{\dot{\boldsymbol{\omega}}}$	$[0, 0, 0]$ deg/sec^2
$\boldsymbol{r}_c$	random as described	$\hat{\boldsymbol{r}}_c$	$[0, 0, 0]$ m
P_{att}	1 deg^2	$P_{\boldsymbol{\omega}}$	$(0.001)^2$ (deg/sec)^2
$P_{\dot{\boldsymbol{\omega}}}$	$(0.001)^2$ (deg/sec)^{22}	$P_{\boldsymbol{r}_c}$	$(0.01)^2$ m^2
$P_{\boldsymbol{a}_b}$	$(0.0001)^2$ (m/sec)^2	$Q_{\boldsymbol{a}_b}$	1×10^{-14} (m/sec)^2
Q_{att}	1×10^{-11} deg^2	$Q_{\boldsymbol{\omega}}$	1×10^{-11} (deg/sec)^2
$Q_{\dot{\boldsymbol{\omega}}}$	1×10^{-11} (deg/sec^2)^2	$Q_{\boldsymbol{r}_c}$	1×10^{-12} m^2
$\sigma_{pulse\ measurement}$	10 μsec	$\sigma_{accelerometer}$	1×10^{-7} m/sec^2
$\sigma_{star,1}$	$[100, 100, 100]$ arc-sec	$\sigma_{sun\ sensor}$	0.1 deg
$\sigma_{star,2}$	$[50, 50, 50]$ arc-sec		

results using the two inertia matrices given in Table 2 and the two star sensor uncertainties given in Table 3 with no accelerometer bias. A solar pressure torque is added to the truth model, but is not considered in the filter model. The truth model torque is given as

$$\mathbf{T} = \boldsymbol{r}_{cp} \times \mathbf{F}_{sun}$$

where $\mathbf{F}_{sun}$ is the solar pressure force and $\boldsymbol{r}_{cp}$ is the vector defining the center of mass to center of pressure. The MMS spacecraft is modeled as a perfect cylinder, with the center of pressure at the geometric center. The vector $\boldsymbol{r}_{cp}$ is therefore the same as $\boldsymbol{r}_c$. The solar pressure force is modeled simply with the following[9]

$$\mathbf{F}_{sun} = \frac{\mathrm{F}_s}{c} A_s (1+q) \hat{\boldsymbol{s}}$$

where F_s=solar constant=1358 W/m^2, c=speed of light=3×10^8 m/sec, A_s= projected area normal to the sun direction, q=reflectance factor=0.6. The unit vector $\hat{\boldsymbol{s}}$ is the vector from the sun to the

spacecraft, providing the direction for $\mathbf{F}_{sun}$ in the spacecraft body frame. The derivative of the torque, $\dot{\mathbf{T}}$, is computed using

$$\dot{\mathbf{T}} = \frac{d\mathbf{T}}{dt}|_B + \boldsymbol{\omega} \times \mathbf{T}$$

The derivative term is computed numerically, and the cross product is computed using the true angular velocity in the body frame. Table 4 gives the averaged final RMS errors for 100 trials, with each trial run for 90 minutes.

Table 4. Average RMS Errors for 100 Trials, Center of Mass Error

Inertia	Star Sensor	$\|\tilde{\boldsymbol{\alpha}}\|$ (deg)	$\|\tilde{\boldsymbol{\omega}}\|$ (deg/sec)	$\tilde{r}_{c,1}$ (cm)	$\tilde{r}_{c,2}$ (cm)	$\tilde{r}_{c,3}$ (cm)
J_1	$\sigma_{star,1}$	0.0084	0.0033	0.0027	0.0030	0.0399
	$\sigma_{star,2}$	0.0053	0.0027	0.0030	0.0032	0.0193
J_2	$\sigma_{star,1}$	0.0081	0.0027	0.0017	0.0021	0.4491
	$\sigma_{star,2}$	0.0051	0.0023	0.0012	0.0014	0.2156

Next the accelerometer bias is considered with no center of mass error (and therefore no solar pressure disturbance torque). The true accelerometer bias is selected from a normal distribution with zero mean and standard deviation of 1×10^{-5} m/sec^2. The initial estimate of $\boldsymbol{a}_b$ is $\hat{\boldsymbol{a}}_b = \begin{bmatrix} 0 & 0 & 0 \end{bmatrix}$ m/sec^2. Table 5 gives the averaged final RMS errors, again for 100 trials with each trial run for 90 minutes.

Table 5. Average RMS Errors for 100 Trials, Accelerometer Bias

Inertia	Star Sensor	$\|\tilde{\boldsymbol{\alpha}}\|$ (deg)	$\|\tilde{\boldsymbol{\omega}}\|$ (deg/sec)	$\tilde{a}_{b,1}$ $(\mu m/sec^2)$	$\tilde{a}_{b,2}$ $(\mu m/sec^2)$	$\tilde{a}_{b,3}$ $(\mu m/sec^2)$
J_1	$\sigma_{star,1}$	0.0067	0.0030	1.162	1.083	1.422
	$\sigma_{star,2}$	0.0046	0.0025	1.155	1.078	0.907
J_2	$\sigma_{star,1}$	0.0060	0.0019	0.894	0.926	1.407
	$\sigma_{star,2}$	0.0041	0.0017	0.653	0.609	0.891

The attitude and rate errors are lower with the accelerometer bias than the center of mass error, given the sizes of the errors applied. Preliminary studies of simultaneously estimating the bias and center of mass indicate a correlation between the two parameters when modeled as a constant. Future work will examine the correlation further and investigate scenarios to improve observability.

CONCLUSION

An Extended Kalman Filter is developed and tested for a single MMS spacecraft. The filter utilizes star sensor, slit sun sensor, and accelerometer measurements. The filter is run for 90 minutes, and each test run is repeated 100 times with different random noise applied to the sensor measurements. Results are presented for two possible inertia configurations, one is for a fully stowed spacecraft and the other is with all extendable booms deployed. Two possible star sensor measurement uncertainties are also considered, 100 and 50 arc-sec, respectively. As expected the results are worse with the higher star sensor uncertainty, however the RMS attitude error degrades by less than

a factor of 2 with the higher measurement uncertainty. First the center of mass location is estimated, along with the attitude, angular velocity, and angular acceleration. In each of the 100 tests, the true center of mass is chosen randomly. The filter successfully estimates the spacecraft attitude, angular velocity, angular acceleration, and center of mass. The worst case RMS attitude error is 30.2 arc-sec, with the fully stowed inertia configuration and star sensor uncertainty of 100 arc-sec. The worst case RMS center of mass error is 0.45 cm in the z body axis direction, for the fully deployed inertia configuration and the 100 arc-sec star sensor uncertainty. The RMS x and y center of mass errors are lower for the fully deployed configuration as compared to the stowed configuration, but the z axis RMS error is larger by an order of magnitude. Next an accelerometer bias is estimated. The worst case RMS attitude error is 24.1 arc-sec for the fully stowed inertia configuration and 100 arc-sec star sensor uncertainty. The worse case accelerometer bias is 1.422 μm/sec^2 in the z body direction for the same scenario. The RMS errors in the accelerometer bias are all lower for the fully deployed configuration as compared to the fully stowed inertia configuration.

Future work will examine the simultaneous estimation of the center of mass and accelerometer bias. Preliminary results indicate a high correlation between both parameters when modeled as constants. An observability analysis will be conducted to determine the extent to which both parameters could be estimated given the current sensor models and spacecraft dynamics.

ACKNOWLEDGMENT

This research was funded by the Magnetospheric Multiscale Mission project, NASA Goddard Space Flight Center, Greenbelt, Maryland.

REFERENCES

[1] Southwest Research, Inc., "MMS Magnetospheric Multiscale Mission," website, mms.space.swri.edu.

[2] Hughes, S. P., "Formation Initial Conditions for Phase I, and Phase IIb, of the Magnetosphere Multiscale Mission (MMS)," Memo, July 2005, Internal NASA Goddard Space Flight Center document.

[3] Markley, F. L., "Attitude Error Representations for Kalman Filtering," *AIAA Journal of Guidance, Control, and Dynamics*, Vol. 26, No. 2, 2003, pp. 311–317.

[4] Bar-Itzhack, I. and Harman, R. R., "Pseudo-Linear Attitude Determination of Spinning Spacecraft," *AIAA Guidance, Navigation, and Control Conference*, Providence, Rhode Island, August 2004.

[5] Kaplan, M. H., *Modern Spacecraft Dynamics and Control*, John Wiley and Sons, Inc., 1976.

[6] Miller, K. S., "On the Inverse of the Sum of Matrices," *Mathematics Magazine*, Vol. 54, No. 2, March 1981, pp. 67–72.

[7] Bryson, A., "Kalman Filter Divergence and Aircraft Motion Estimator," *Journal of Guidance and Control*, Vol. 1, No. 1, January-February 1978, pp. 71–79.

[8] Olney, D., "MMS Attitude Control Analysis Report," Report, July 2008, Calculation of MMS Principal Axes Offsets.

[9] Wertz, J. R. and Larson, W. J., *Space Mission Analysis and Design*, Microcosm Press and Kluwer Academic Publishers, 1999.

APPENDIX A: DEVELOPMENT OF PARTIAL DERIVATIVES

Let

$$\mathrm{v}_1 = \mathrm{J}_{\boldsymbol{r}_c}[[\boldsymbol{\omega}\times]\mathrm{J}_\mathrm{B}\dot{\boldsymbol{\omega}} + [\dot{\boldsymbol{\omega}}\times]\mathrm{J}_\mathrm{B}\boldsymbol{\omega}]$$
$$\mathrm{v}_2 = [\boldsymbol{\omega}\times][\boldsymbol{r}_c\times]^2\dot{\boldsymbol{\omega}} + [\dot{\boldsymbol{\omega}}\times][\boldsymbol{r}_c\times]^2\boldsymbol{\omega}$$
$$\mathrm{v}_3 = \mathrm{J}_{\boldsymbol{r}_c}[[\boldsymbol{\omega}\times][\boldsymbol{r}_c\times]^2\dot{\boldsymbol{\omega}} + [\dot{\boldsymbol{\omega}}\times][\boldsymbol{r}_c\times]^2\boldsymbol{\omega}]$$

Then

$$\mathrm{F}_{\ddot{\boldsymbol{\omega}},\boldsymbol{r}_c} = \mathrm{J}_\mathrm{B}{}^{-1}\frac{\partial \mathrm{v}_1}{\partial \boldsymbol{r}_c} + m\mathrm{J}_\mathrm{B}{}^{-1}\frac{\partial \mathrm{v}_2}{\partial \boldsymbol{r}_c} - m\mathrm{J}_\mathrm{B}{}^{-1}\frac{\partial \mathrm{v}_3}{\partial \boldsymbol{r}_c}$$

Partial Derivative of v_1

The vector v_1 is given as

$$\mathrm{v}_1 = \mathrm{J}_{\boldsymbol{r}_c}[[\boldsymbol{\omega}\times]\mathrm{J}_\mathrm{B}\dot{\boldsymbol{\omega}} + [\dot{\boldsymbol{\omega}}\times]\mathrm{J}_\mathrm{B}\boldsymbol{\omega}] = \mathrm{J}_{\boldsymbol{r}_c}\mathrm{v}_\omega$$

where $\mathrm{v}_\omega = [\boldsymbol{\omega}\times]\mathrm{J}_\mathrm{B}\dot{\boldsymbol{\omega}} + [\dot{\boldsymbol{\omega}}\times]\mathrm{J}_\mathrm{B}\boldsymbol{\omega}$ and is not dependent on $\boldsymbol{r}_c$. Recall that $\mathrm{J}_{\boldsymbol{r}_c}$ is

$$\mathrm{J}_{\boldsymbol{r}_c} = \frac{1}{a+b}(a\mathrm{G} - \mathrm{G}^2)$$

The matrix G is given as

$$\mathrm{G} = -m[\boldsymbol{r}_c\times]^2{\mathrm{J}_\mathrm{B}}^{-1}$$

and $a = trace(\mathrm{G})$ and $2b = (trace(\mathrm{G}))^2 - trace(\mathrm{G}^2)$. The partial derivative matrix is then

$$\frac{\partial \mathrm{v}_1}{\partial \boldsymbol{r}_c} = \left[\begin{array}{c:c:c} (\frac{\partial}{\partial r_{c,1}}\mathrm{J}_{\boldsymbol{r}_c})\mathrm{v}_\omega & (\frac{\partial}{\partial r_{c,2}}\mathrm{J}_{\boldsymbol{r}_c})\mathrm{v}_\omega & (\frac{\partial}{\partial r_{c,3}}\mathrm{J}_{\boldsymbol{r}_c})\mathrm{v}_\omega \end{array}\right]$$

where $r_{c,i}$ are the 3 elements of $\boldsymbol{r}_c$. The partial derivatives of the elements of $\mathrm{J}_{\boldsymbol{r}_c}$ are

$$\frac{\partial \mathrm{J}_{\boldsymbol{r}_c}{}_{j,k}}{\partial r_{c,i}} = \frac{1}{a+b}(\frac{\partial a}{\partial r_{ci}}\mathrm{G}_{j,k} + a\frac{\partial \mathrm{G}_{j,k}}{\partial r_{ci}} - \frac{\partial}{\partial r_{ci}}\sum_{l=1}^{3}\mathrm{G}_{j,l}\mathrm{G}_{l,k}) - \frac{(a\mathrm{G}_{j,k} - \mathrm{G}^2_{j,k})\frac{\partial(a+b)}{\partial r_{ci}}}{(a+b)^2}$$

where $j = 1,2,3$ and $k = 1,2,3$ to cover all 9 elements in $\mathrm{J}_{\boldsymbol{r}_c}$, $\mathrm{G}_{j,k}$ are the elements of G, and $\mathrm{G}^2_{j,k}$ are the elements of the matrix G^2. The partial derivatives of all the elements in G with respect to each element of $\boldsymbol{r}_c$ are computed as

$$\frac{\partial}{\partial r_{c,i}}\mathrm{G} = -m(\frac{\partial}{\partial r_{c,i}}[\boldsymbol{r}_c\times]^2){\mathrm{J}_\mathrm{B}}^{-1}$$

The matrix $[\boldsymbol{r}_c\times]^2$ is

$$[\boldsymbol{r}_c\times]^2 = \boldsymbol{r}_c\boldsymbol{r}_c^T - \|\boldsymbol{r}_c\|^2\mathrm{I}$$

Therefore

$$\frac{\partial[\boldsymbol{r}_c\times]^2}{\partial r_{c,i}} = \boldsymbol{e}_i\boldsymbol{r}_c^T + \boldsymbol{r}_c\boldsymbol{e}_i^T - 2\boldsymbol{r}_c\mathrm{I}$$

where $\boldsymbol{e}_i$ is the ith body axis unit vector. The partial derivative of a with respect to $\boldsymbol{r}_c$ is

$$\frac{\partial a}{\partial r_{ci}} = \frac{\partial \mathrm{G}_{1,1}}{\partial r_{ci}} + \frac{\partial \mathrm{G}_{2,2}}{\partial r_{ci}} + \frac{\partial \mathrm{G}_{3,3}}{\partial r_{ci}}$$

The partial derivative of $a+b$ with respect to $\boldsymbol{r}_c$ is

$$\frac{\partial(a+b)}{\partial r_{ci}} = a\frac{\partial a}{\partial r_{ci}} - \sum_{j=1}^{3}\sum_{k=1}^{3}\mathrm{G}_{j,k}\frac{\partial \mathrm{G}_{k,j}}{\partial r_{ci}}$$

Partial Derivative of v_2

The vector v_2 is given as

$$\mathrm{v}_2 = [\boldsymbol{\omega}\times][\boldsymbol{r}_c\times]^2\dot{\boldsymbol{\omega}} + [\dot{\boldsymbol{\omega}}\times][\boldsymbol{r}_c\times]^2\boldsymbol{\omega}$$

The partial derivative matrix is

$$\frac{\partial \mathrm{v}_2}{\partial \boldsymbol{r}_c} = \begin{bmatrix} \frac{\partial \mathrm{v}_2}{\partial r_{c,1}} & \vdots & \frac{\partial \mathrm{v}_2}{\partial r_{c,2}} & \vdots & \frac{\partial \mathrm{v}_2}{\partial r_{c,3}} \end{bmatrix}$$

where

$$\frac{\partial \mathrm{v}_2}{\partial r_{c,i}} = [\boldsymbol{\omega}\times](\frac{\partial}{\partial r_{c,i}}[\boldsymbol{r}_c\times]^2)\dot{\boldsymbol{\omega}} + [\dot{\boldsymbol{\omega}}\times](\frac{\partial}{\partial r_{c,i}}[\boldsymbol{r}_c\times]^2)\boldsymbol{\omega}$$

Partial Derivative of v_3

The vector v_3 is

$$\mathrm{v}_3 = \mathrm{J}_{\boldsymbol{r}_c}[[\boldsymbol{\omega}\times][\boldsymbol{r}_c\times]^2\dot{\boldsymbol{\omega}} + [\dot{\boldsymbol{\omega}}\times][\boldsymbol{r}_c\times]^2\boldsymbol{\omega}] = \mathrm{J}_{\boldsymbol{r}_c}\mathrm{v}_2$$

The partial derivative matrix is

$$\frac{\partial \mathrm{v}_3}{\partial \boldsymbol{r}_c} = \begin{bmatrix} \frac{\partial \mathrm{v}_3}{\partial r_{c,1}} & \vdots & \frac{\partial \mathrm{v}_3}{\partial r_{c,2}} & \vdots & \frac{\partial \mathrm{v}_3}{\partial r_{c,3}} \end{bmatrix}$$

where the columns are computed as

$$\frac{\partial \mathrm{v}_3}{\partial r_{c,i}} = \frac{\partial \mathrm{J}_{\boldsymbol{r}_c}}{\partial r_{c,i}}\mathrm{v}_2 + \mathrm{J}_{\boldsymbol{r}_c}\frac{\partial \mathrm{v}_2}{\partial r_{c,i}}$$